

Author Manuscript

Title: A MOF Multifunctional Cargo Vehicle for Reactive Gas Delivery and Catalysis

Authors: Preecha Kittikhunnatham, Ph.D.; Gabrielle A. Leith; Abhijai Mathur; Jennifer K. Naglic; Corey R. Martin; Kyoung Chul Park; Katherine McCullough, Ph.D.; H. D. A. Chathumal Jayaweera; Ryan E. Corkill; Jochen Lauterbach, Ph.D.; Stavros G. Karakalos, Ph.D.; Mark D. Smith, Ph.D.; Sophya Garashchuk, Ph.D.; Donna A. Chen, Ph.D.; Natalia B. Shustova, Ph.D.

This is the author manuscript accepted for publication. It has not been through the copyediting, typesetting, pagination and proofreading process, which may lead to differences between this version and the Version of Record.

To be cited as: 10.1002/anie.202113909

Link to VoR: https://doi.org/10.1002/anie.202113909

A MOF Multifunctional Cargo Vehicle for Reactive-Gas Delivery and Catalysis

Preecha Kittikhunnatham, [a] Gabrielle A. Leith, [a] Abhijai Mathur, [a] Jennifer K. Naglic, [b] Corey R. Martin, [a] Kyoung Chul Park, [a] Katherine McCullough, [b] H. D. A. Chathumal Jayaweera, [a] Ryan E. Corkill, [a] Jochen Lauterbach, [b] Stavros G. Karakalos, [b] Mark D. Smith, [a] Sophya Garashchuk, [a] Donna A. Chen,*[a] Natalia B. Shustova*[a]

- Dr. P. Kittikhunnatham, G. A. Leith, A. Mathur, C. R. Martin, K. C. Park, H. D. A. C. Jayaweera, R. E. Corkill, Dr. M. D. Smith, Prof. Dr. S. Garashchuk, Prof. Dr. D. A. Chen, Prof. Dr. N. B. Shustova Department of Chemistry and Biochemistry
 - University of South Carolina Columbia, SC 29208 (USA)

RESEARCH ARTICLE

E-mail: shustova@sc.edu

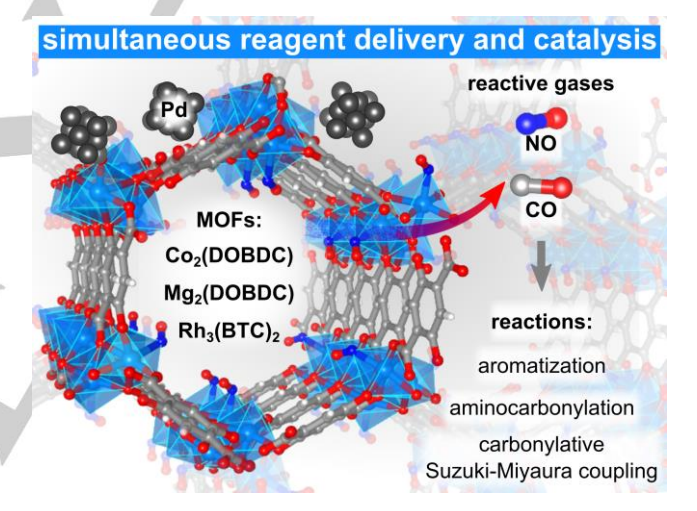
J. K. Naglic, Dr. K. McCullough, Prof. Dr. J. Lauterbach, Dr. S. G. Karakalos Department of Chemical Engineering University of South Carolina Columbia, SC 29208 (USA)

Supporting information for this article is given via a link at the end of the document.

Abstract: Efficient delivery of reactive and toxic gaseous reagents to organic reactions was studied using metal-organic frameworks (MOFs). Simultaneous cargo vehicle and catalytic capabilities of several MOFs were probed for the first time using the examples of aromatization, aminocarbonylation, and carbonylative Suzuki-Miyaura coupling reactions. These reactions highlight that MOFs can serve a dual role as a gas cargo vehicle and a catalyst, leading to product formation with yields similar to reactions employing pure gases. Furthermore, the MOFs can be recycled without sacrificing product yield, while simultaneously maintaining crystallinity. The reported findings were supported crystallographically and spectroscopically (e.g., diffuse reflectance infrared Fourier transform spectroscopy), foreshadowing a pathway for the development of multifunctional MOF-based reagent-catalyst cargo vessels for reactive reagents, as an attractive alternative to the use of toxic pure gases or gas generators.

Introduction

Toxic gases such as carbon monoxide and nitric oxide are desirable chemical reagents for the synthesis of many high-value pharmaceuticals (e.g., ketoprofen, olaparib, thalidomide, fenofibrate, or decimemide), drug precursors (e.g., nordazepam, florbetaben, or clenbuterol), or for synthesizing precursors of complex molecules used in chemical, agrochemical, and pharmaceutical industries.[1-6] However, both NO and CO are reactive gases with low lethal doses and IDLH (immediately dangerous to life or health concentrations) of 100 and 1200 ppm, respectively. Due to their toxicity and reactivity, expensive safety measures are required to handle, store, and transport these gases safely, thereby placing their usage in synthetic chemistry under strict regulations.[7] Herein, we probed metal-organic frameworks (MOFs),[8-33] specifically their reversible gas adsorption and catalytic activity, to carry out chemical reactions in organic solvents. Thus, we explored the dual role of MOFs as a catalyst and carrier of reagents on the example of reactive gases.



Scheme 1. A schematic representation of a synergistic MOF-based platform used in the current studies for gaseous reagent delivery and catalysis to carry out organic reactions including aromatization, aminocarbonylation, and carbonylative Suzuki-Miyaura coupling.

To the best of our knowledge, utilization of MOFs for organic synthesis as CO/NO reagent carriers has not been explored thus far, and particularly the presented concept of combining the catalytic properties of MOFs with CO (or NO) delivery has not been reported (Scheme 1). Previous studies of nitric oxide and carbon monoxide adsorption on framework metal sites, [34-37] that were used for signaling processes in cells using CO(NO) as gasotransmitters,[37-43] have laid the foundation for the studies herein. In contrast to previous reports, we surveyed MOFs as carriers for reactive NO and CO to carry out transition-metalcatalyzed aminocarbonylation, carbonylative Suzuki-Miyaura coupling, and aromatization reactions for the preparation of, for example, thalidomide (that is used to treat leprosy and cancerous tumors) or 2-amino-5-chlorobenzophenone (a building block for nordazepam, an anxiety disorder medication). [44,45] As shown below, utilization of gas@MOF solid samples as reagents could lead to the same level of product conversion and yields compared to direct NO and CO gas usage. Furthermore, the use of gas@MOFs instead of molecular in situ CO generators, that typically require byproduct extraction, [46-48] enables isolation of the used MOF carriers without column chromatography, simply through gravity filtration, allowing us to probe the recyclability of the prepared frameworks. Prior to examining the gas delivery capacity, the selected frameworks underwent a comprehensive analysis using single-crystal and powder X-ray diffraction (SC-XRD and PXRD, respectively), thermogravimetric analysis (TGA), attenuated total reflection-Fourier transform infrared (ATR-FTIR) spectroscopy, diffuse reflectance infrared Fourier transform spectroscopy (DRIFTS), diffuse reflectance (DR) and energydispersive X-ray (EDX) spectroscopies, inductively coupled plasma mass spectrometry (ICP-MS), and theoretical calculations. Despite high-temperature activation (up to 250 °C) and reactive gas exposure, we were able to study the coordination of a reactive gas (NO) to the metal sites of the MOF through SC-XRD for the first time (Figure 1). Throughout the studies, the framework integrity was carefully monitored crystallographically and spectroscopically.

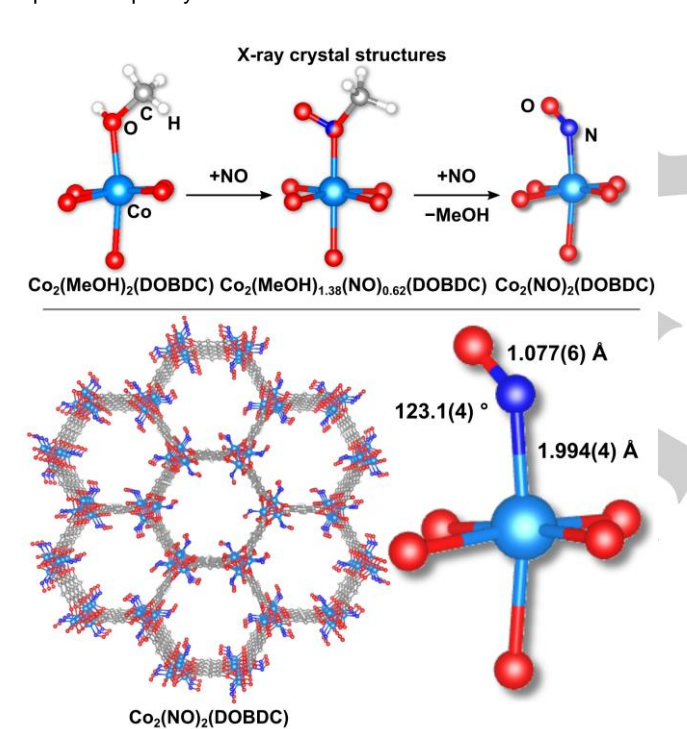


Figure 1. (top) Crystallographically-resolved changes in metal node coordination environment of $Co_2(DOBDC)$ upon exposure to NO gas, displaying a stepwise replacement of methanol molecules (solvent) with NO. (bottom left) X-ray crystal structure of $Co_2(NO)_2(DOBDC)$ with coordinated NO molecules. The light blue, dark blue, gray, red, and white spheres represent cobalt, nitrogen, carbon, oxygen, and hydrogen atoms, respectively. (bottom right) Secondary building unit (SBU) of $Co_2(NO)_2(DOBDC)$ as well as the Co-NO (1.994(4) Å) and average N-O (1.077(6) Å) distances and the Co-N-O (123.1(4)°) angle are highlighted.

Results and Discussion

Herein we explore two concepts: (1) utilizing the framework for delivery of reactive and lethal gases, such as CO and NO, for

performing organic transformations in solution and (2) testing the dual role of MOFs as a catalyst and a gas carrier. To the best of our knowledge, these two concepts have not been applied for carbon monoxide and nitric oxide gases as reagents. We used previous reports on the binding of CO (or NO) gases to the unsaturated metal sites and gas release kinetics in biologically relevant processes as a basis for our studies. [34-43,49,50] The initial selection of three MOFs was performed based on their structural and thermal stability, relatively high gas adsorption capacity, and reversible gas binding capability. Both Mg2(DOBDC) and Co₂(DOBDC) (H₄DOBDC = 2,5-dioxido-1,4-benzenedicarboxylic acid) are isostructural (rhombohedral, a = b = 26.02(1) Å and c =6.721(4) Å for Co₂(DOBDC); structural features are shown in Figure 1).[34,51-53] According to our analysis, the Mg- and Cocontaining MOFs are thermally stable up to 250 °C and 180 °C under vacuum, respectively (Figure S2). Their exceptional thermal stability facilitates and simplifies their activation procedures.[34,35,51] At the same time, these MOFs also possess relatively high CO adsorption capacities of 4.58 mmol/g (for Mg₂(DOBDC)) and 5.95 mmol/g (Co₂(DOBDC) at 1.2 bar (298 K). respectively.[34] For gaining a better understanding and comparing the frameworks used in these studies, we estimated the binding energy of CO (and NO) to the metal nodes using density functional theory (DFT) calculations (Figure 2 and Table S2). Notably, some of the binding energies were estimated before; [34] however, comparison of the frameworks (selected in this work) with each other requires the calculations to be performed for all MOFs using the same density functional and basis set. After considering three commonly used density functionals, i.e., B3LYP-D3, MO6-2X, and ω B97X-D, B3LYP-D3 was employed for most of the calculations. A detailed description of the computational aspects is provided in the supporting information (SI). [54-56] The binding energies were estimated to be 40.3 kJ/mol and 39.7 kJ/mol for CO bound to the metal center in Mg₂(DOBDC) and Co₂(DOBDC), and the corresponding Mg-CO and Co-CO bond lengths were estimated to be 2.54 and 2.27 Å, respectively (Figure 2 and Table S2).

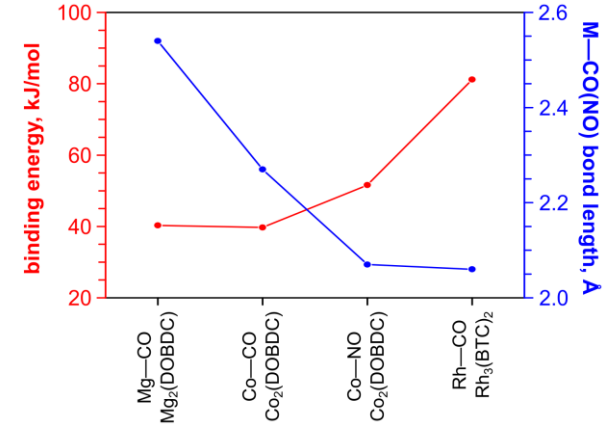


Figure 2. Calculated binding energy of CO and NO to the metal nodes (red) and metal–NO and metal–CO bond lengths (blue) in MOFs chosen for this work. Binding energies were calculated using the B3LYP-D3 density functional paired with the 6-31+G** basis and corrected with ZPE, and bond lengths were computed at the B3LYP/6-31G* level.

Preparation of $M_2(DOBDC)$ (M = Mg and Co) frameworks was performed by heating the corresponding M(NO₃)₂ salts and H₄DOBDC in a DMF/ethanol/water mixture at 125 °C for 20 hours (Mg(NO₃)₂) or at 100 °C for 24 hours (Co(NO₃)₂), see the SI for more details.[34,51] We demonstrated reversible room temperature binding of CO to Co₂(DOBDC) metal sites using DRIFTS for the first time (Figure 3). The DRIFTS spectra of Co₂(DOBDC) in the presence of CO revealed a growth in the C-O stretching frequency at 2156 cm⁻¹, that is higher than that of noncoordinated CO (2143 cm⁻¹), [58] and is in line with previous reports indicating no significant π -backdonation.^[34,59] Moreover, the observed findings are in agreement with literature reports (2164 cm⁻¹).^[34] As a next step, we tested the reversibility of CO binding. For that, we recorded the DRIFTS spectra during intensive purging of the CO@Co2(DOBDC) sample with nitrogen for 150 minutes. Indeed, a decrease in the C-O band intensity (2156 cm-1) over time was detected (Figure 3, see more details in the SI), confirming reversible binding of carbon monoxide to the MOF metal sites. Such reversible binding capacity was crucial for our studies since CO should not only coordinate to the metal center. but also be released during the organic reactions. Notably, our investigations of the Mg₂(DOBDC) system is in line with a previous report.[34]

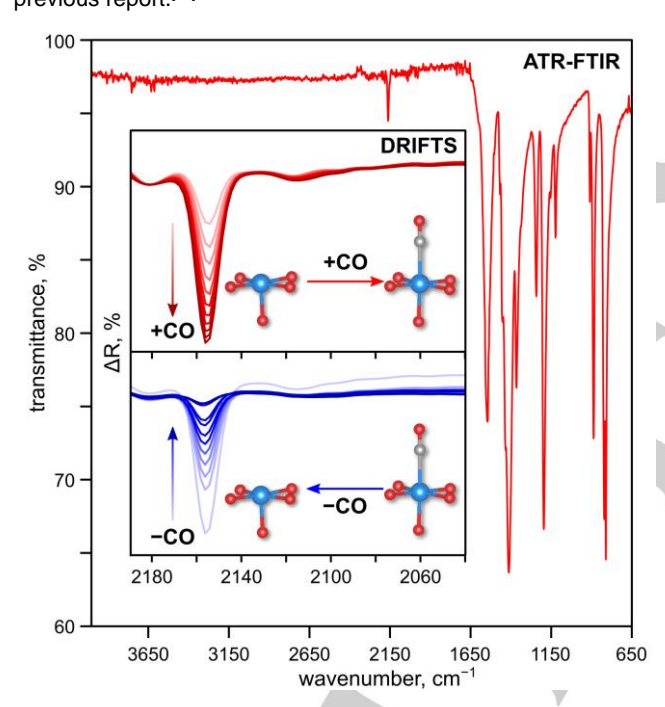


Figure 3. The ATR-FTIR spectrum of CO@Co₂(DOBDC) (red). The top inset shows DRIFTS spectra of Co₂(DOBDC) (red) collected at room temperature in the presence of carbon monoxide. The bottom inset demonstrates changes in the DRIFT spectra (% differential reflection (ΔR)) of CO@Co₂(DOBDC) (blue) upon intensive sample purging with nitrogen. A schematic representation of CO coordination and dissociation processes is provided. The light blue, gray, and red spheres represent cobalt, carbon, and oxygen atoms, respectively. Hydrogen atoms are omitted for clarity.

As test reactions with CO gas, we chose to synthesize thalidomide and nordazepam precursors (valuable pharmaceuticals) $^{[2,3]}$ as a proof-of-principle that the developed approach could be used for synthesizing commodity chemicals. Initially, we carried out the aminocarbonylation reaction by using Mg₂(DOBDC) as a cargo vehicle for CO delivery (Figure 4). For

that, Mg₂(DOBDC), was first activated at 250 °C for 3 hours under dynamic vacuum, then exposed to CO at 77 K (a more detailed procedure can be found in the SI), and the produced CO@Mg₂(DOBDC) sample was stored at room temperature under a CO atmosphere. Preservation of Mg₂(DOBDC) crystallinity after CO exposure was evaluated by PXRD, confirming the integrity of the Mg₂(DOBDC) framework (Figure 4). After performing several control experiments in the absence of carbon monoxide or in the presence of Mg₂(DOBDC) (instead of CO@Mg₂(DOBDC), see more details in the SI), the prepared CO@Mg₂(DOBDC) framework was used as a CO source in the aminocarbonylation reaction.

Mg₂(DOBDC)

carbonylative Suzuki-Miyaura coupling

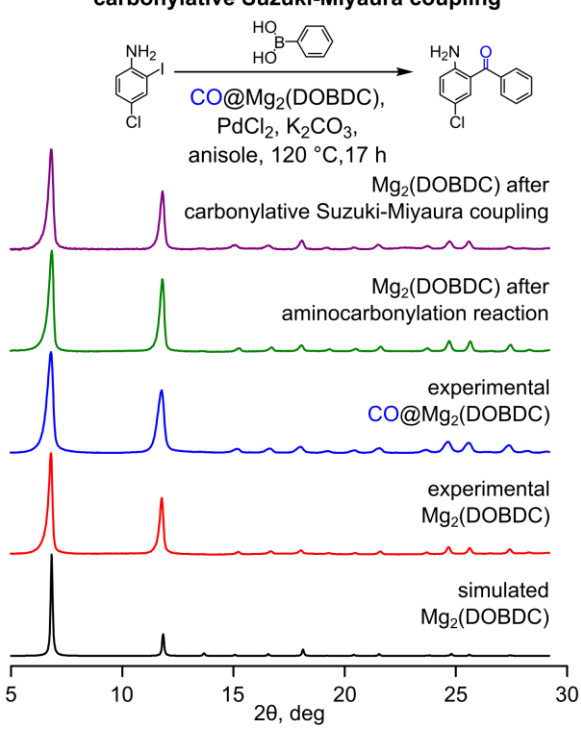


Figure 4. (*top*) Examples of organic reactions explored in the current work using CO@Mg₂(DOBDC) as a gaseous reagent delivery vehicle. (*bottom*) PXRD patterns of Mg₂(DOBDC): simulated (black), as-synthesized (red), experimental after CO exposure (blue), isolated after utilization in the aminocarbonylation reaction (green), and isolated after utilization in the carbonylative Suzuki-Miyaura coupling reaction (purple).

For that, 2-bromo-N-(2,6-dioxopiperidin-3-yl)benzamide, 4-dimethylaminopyridine (DMAP), 4,5-bis(diphenylphospheno)-9,9-dimethyl xanthene (Xantphos), and bis(dibenzylideneacetone)palladium (Pd(dba)₂) were added to the prepared CO@Mg₂(DOBDC) framework in a Schlenk flask under positive nitrogen pressure (Figure 5). Anhydrous anisole and N,N-diisopropylethylamine (DIPEA) were added to the flask, followed by heating at 100 °C for 21 hours, resulting in the formation of thalidomide in 56% yield (Figures S3 and S4). As a

control experiment, we carried out the same reaction under identical reaction conditions but instead of CO@Mg2(DOBDC), we used CO gas. Remarkably, the acquired yield using CO@Mg2(DOBDC) (56%) was practically identical to the one obtained under the same reaction conditions but with CO gas (58%). Product conversion was controlled through the number of moles of CO added to the mixture (i.e., mass of CO@framework). Figure 5 contains ¹H NMR spectra of the crude reaction mixtures from the aminocarbonylation reaction using 3.53 equivalents of CO@Mg2(DOBDC) (ca. 3.68 equivalents of CO) and 1.38 equivalents of CO@Mg2(DOBDC) (ca. 1.44 equivalent of CO) as reagents. The ¹H NMR spectrum of the isolated reaction mixture, carried out with 1.38 equivalents of CO@Mg2(DOBDC), contained prominent resonances at δ = 10.87 ppm corresponding to the starting material, 2-bromo-N-(2,6-dioxopiperidin-3yl)benzamide, and a resonance at δ = 11.15 ppm, corresponding to the product, thalidomide (Figure 5). In contrast, performing the reaction with 3.53 equivalents of CO@Mg2(DOBDC) led to almost 100% conversion. Therefore, loading a sufficient amount of CO into the MOF is an important parameter to consider when performing these reactions (see the SI for more details). The

RESEARCH ARTICLE

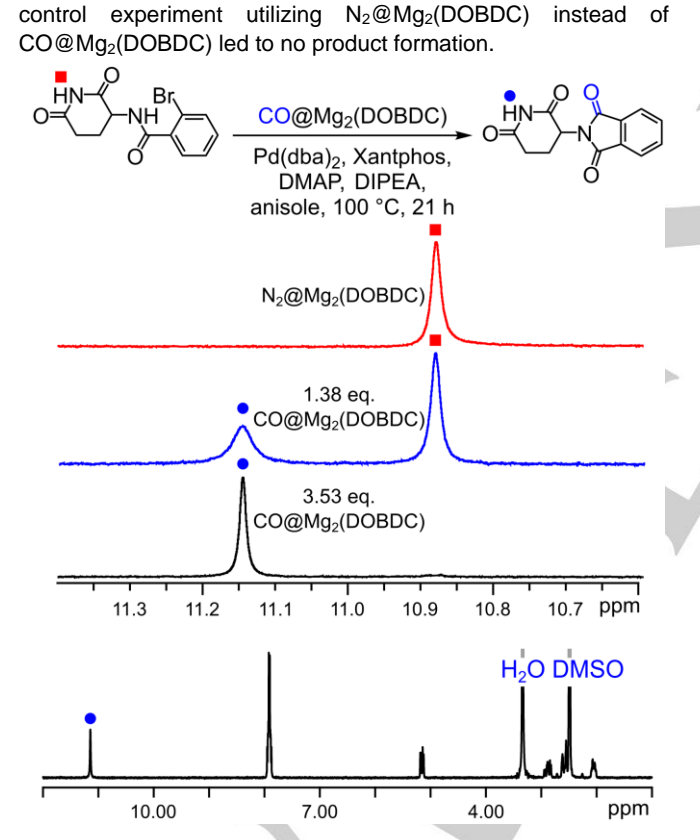


Figure 5. (top) Reaction scheme for the aminocarbonylation reaction using CO@Mg₂(DOBDC). (middle) ¹H NMR spectra collected of crude products obtained from the control reaction using N2@Mg2(DOBDC) (red), using 1.38 equivalents of CO@Mg2(DOBDC) (blue), and using 3.53 equivalents of CO@Mg2(DOBDC) (black). (bottom) 1H NMR spectrum of the product, thalidomide, prepared from the reaction using CO@Mg2(DOBDC). The peaks corresponding to the starting material (■) and the product (●) are labeled.

As a next step, we evaluated the crystallinity of Mg₂(DOBDC) after CO delivery and exposure to the reaction conditions (Figure 4). The MOF was first thoroughly washed with ethyl acetate and methanol using a Soxhlet apparatus to ensure the removal of any

Co₂(DOBDC) aminocarbonylation CO@Co₂(DOBDC) Pd(dba)₂, Xantphos, DMAP, DIPEA, anisole, 100 °C, 21 h carbonylative Suzuki-Miyaura coupling CO@Co2(DOBDC), PdCl₂, K₂CO₃, anisole, 120 °C, 17 h aromatization NO@Co2(DOBDC) air, benzene, H2O r.t., 20 min Co₂(DOBDC) after aromatization reaction (air and water) Co₂(DOBDC) after aromatization reaction (water) Co₂(DOBDC) after aromatization reaction (air) Co₂(DOBDC) after aromatization reaction (anaerobic) experimental NO@Co2(DOBDC) Co₂(DOBDC) after carbonylative Suzuki-Miyaura coupling Co₂(DOBDC) after aminocarbonylation reaction experimental CO@Co₂(DOBDC) experimental Co₂(DOBDC) simulated Co₂(DOBDC)

Figure 6. (top) Examples of organic reactions explored in the current work using Co₂(DOBDC) as a gaseous reagent delivery vehicle. (bottom) PXRD patterns of Co₂(DOBDC): simulated (black), as-synthesized (red), experimental after CO exposure (blue), isolated after utilization in the aminocarbonylation reaction (green), isolated after its use in the carbonylative Suzuki-Miyaura coupling reaction (purple), experimental Co₂(DOBDC) after NO exposure (orange), and isolated after utilization in the aminocarbonylation reaction with different conditions: without air and water (yellow), with air (pink), with water (maroon), and with air and water (olive).

2θ, deg

20

15

25

30

10

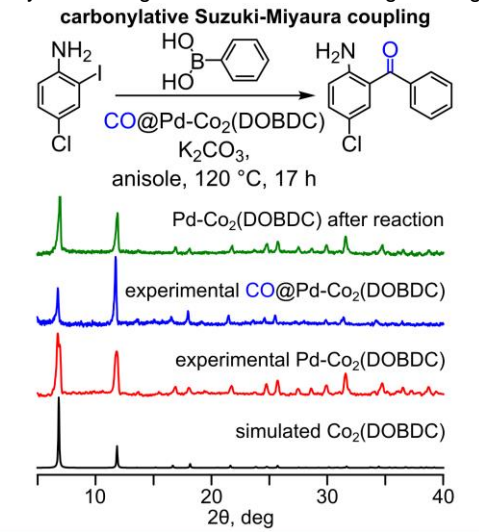
residual components from the reaction mixture. As shown in Figure 4, the collected PXRD pattern demonstrated preservation of framework crystallinity and integrity after the reaction and the extensive washing procedure.

As another framework for CO delivery, we explored Co₂(DOBDC) (Figure 6).^[34,35,51,53,60] Due to a larger CO absorption capacity (5.95 mmol/g at 1.2 bar (298 K))[34] and similar CO binding capability (binding energy = 39.7 kJ/mol, based on DFT calculations; Figure 2 and Table S2) in comparison with Mg₂(DOBDC), we hypothesized that CO@Co₂(DOBDC) could be an even more attractive candidate for practical applications. For instance, the ATR-FTIR spectrum of CO@Co2(DOBDC), stored in a sealed ampule for one week at room temperature, demonstrated preservation of the C-O stretching frequency at 2160 cm⁻¹, corresponding to CO bound to the framework metal sites, indicating that CO can be stored within Co₂(DOBDC) (Figure S5). We then used CO@Co2(DOBDC) as a source of CO to perform an aminocarbonylation reaction of 2-bromo-N-(2,6dioxopiperidin-3-yl)benzamide, using similar conditions to the same reaction with CO@Mg2(DOBDC) (see the SI for more details), resulting in the preparation of thalidomide with 67% yield (Figure 6). After being used as the CO delivery vessel, the MOF was separated by filtration and thoroughly washed with ethyl acetate and methanol using a Soxhlet apparatus to ensure the removal of any residual components from the reaction mixture. The collected PXRD pattern of the washed MOF (Figure 6) demonstrated preservation of framework crystallinity and integrity after the reaction and subsequent extensive washing procedure. Due to the observed remarkable framework stability, we also explored the possibility to recycle the used Co₂(DOBDC) for a second time under the same experimental conditions. As a result, we observed formation of the product without sacrificing the yield (more details can be found in the SI). The recovered Cocontaining MOF still demonstrated crystallinity and preservation of its integrity, providing a pathway for its reusability in multiple cycles (Figure S6). Thus, both Mg₂(DOBDC) and Co₂(DOBDC) can be utilized as a safe vessel for CO delivery without compromising the product yield.

A second reaction that was probed using DOBDC-based MOFs as CO carriers was a carbonylative Suzuki-Miyaura synthesis reaction for the of coupling chlorobenzophenone^[3] (Figures 4 and 6). The CO@M₂(DOBDC) (M = Mg or Co) samples prepared for CO delivery were synthesized using the same procedure as described above. To carry out this reaction, phenylboronic acid, 4-chloro-2-iodoaniline, potassium carbonate, and palladium(II) chloride (PdCl₂) were added to $CO@M_2(DOBDC)$ (M = Mg or Co) in a Schlenk flask under positive nitrogen pressure. After the addition of anhydrous anisole as the solvent, the reaction mixture was heated in a Schlenk flask at 120 °C for 17 hours, resulting in the formation of 2-amino-5-chlorobenzophenone utilizing CO@Co₂(DOBDC) (45% yield) and CO@Mg₂(DOBDC) (49% yield). To explore the concept of MOF recyclability after CO delivery, the MOF was first thoroughly washed with ethyl acetate and methanol using a Soxhlet apparatus to remove any residual compounds. The PXRD patterns of the washed MOFs show that the crystallinity and integrity of the frameworks were preserved (Figure 6). The isolated yield using the CO@MOFs instead of CO was relatively low in comparison with CO gas (75%) and literature reports utilizing CO generators (62%).[3]

For a framework with a higher CO binding energy (81.2 kJ/mol) in comparison with $M_2(DOBDC)$ MOFs (M = Mg or Co), we chose $Rh_3(BTC)_2$ ($H_3BTC=1,3,5$ -benzenetricarboxylic acid) to efficiently adsorb CO, based on reports by the Fischer group. [61,62] Notably, $Rh_3(BTC)_2$ can also act as a catalyst in

hydrogenation and ethylene dimerization reactions.[61,63] The Rh₃(BTC)₂ framework was prepared using a reported procedure, [62] and the carbonylative Suzuki-Miyaura coupling reaction was carried out under the same experimental conditions employed for CO@Mg2(DOBDC) and CO@Co2(DOBDC) (vide supra), but using CO@Rh₃(BTC)₂ as the CO carrier. As expected, the use of Rh₃(BTC)₂ for CO delivery resulted in the formation of 2-amino-5-chlorobenzophenone with 22% yield, but the isolated MOF after the reaction did not maintain its integrity according to PXRD analysis (Figure S7). Notably, we detected product formation using CO@Rh3(BTC)2, even in the absence of the catalyst (PdCl₂), under the same experimental conditions used in the case of $M_2(DOBDC)$ (M = Mg and Co). One possible hypothesis for such behavior is that the Rh₃(BTC)₂ framework degraded and resulted in the formation of metal particles that could catalyze the Suzuki-Miyaura coupling reaction. To test this hypothesis, we prepared a more robust heterometallic isostructural analog, Cu_{2.38}Rh_{0.62}(BTC)₂, using a literature procedure, [64] that could maintain its crystallinity after the reaction (Figure S8). Indeed, PXRD analysis revealed Cu_{2,38}Rh_{0,62}(BTC)₂ could be isolated after the reaction and retained its structural integrity (Figure S8). As expected, due to framework stability (and the absence of decomposition products), product formation observed no was CO@Cu_{2,38}Rh_{0,62}(BTC)₂; however, the use CO@Cu_{2,38}Rh_{0,62}(BTC)₂ in the presence of the PdCl₂ catalyst resulted in the formation of the product. A detailed synthetic procedure and characterization of Cu_{2.38}Rh_{0.62}(BTC)₂ is described in the SI. To further elaborate on the possible dual role of a MOF performing as a gas carrier and catalyst, we prepared the robust Co₂(DOBDC) framework (that preserved its integrity under the reaction conditions as shown above) containing impregnated Pd nanoparticles to carry out the Suzuki-Miyaura coupling reaction (Figure 7). We hypothesized that Co₂(DOBDC) would act as a CO carrier, as shown above, while the Pd particles could catalyze the formation of 2-amino-5-chlorobenzophenone. Pd nanoparticle impregnation within the framework matrix was performed using a literature procedure. [65] As shown in Figure 7, elemental mapping via EDX spectroscopy indicated Pd-particle dispersion, and the EDX data indicated the presence of Pd species with an atomic percentage of 4.4% (Figure S9), which is in agreement with the results obtained from the ICP-MS data (4.0%). Moreover, PXRD analysis demonstrated the structural integrity of the framework after Pd impregnation (Figure 7). The synthesis of 2-amino-5chlorobenzophenone with CO@Pd-Co2(DOBDC) was carried out under the same experimental conditions as described above; phenylboronic acid, 4-chloro-2-iodoaniline, and potassium carbonate were added to CO@Pd-Co2(DOBDC) in a Schlenk flask under positive nitrogen pressure. After the addition of anhydrous anisole as the solvent, the reaction mixture was heated in a Schlenk flask at 120 °C for 17 hours, but without the presence of the PdCl₂ catalyst. The observed yield (42%) was similar to that of the reaction that used PdCl2 as a catalyst and CO@Co₂(DOBDC) (45% yield) as a source of CO. The control experiment in which only CO@Co2(DOBDC) was used (without the presence of any Pd-containing species) did not demonstrate the formation of the desired product. After the reaction, the used Pd-containing MOF was collected via gravity filtration, and the PXRD analysis of Pd-Co₂(DOBDC) demonstrated that the isolated framework maintained its crystallinity after being exposed to the reaction conditions (Figure 7). Thus, these studies showcase that the CO@Pd-Co₂(DOBDC) framework can serve as a catalyst and reagent carrier without losing its integrity.



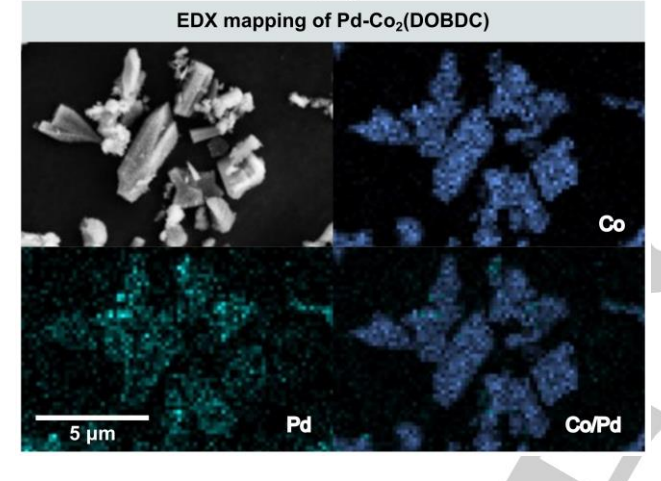


Figure 7. (*top*) Reaction scheme for carbonylative Suzuki-Miyaura coupling using CO@Pd-Co₂(DOBDC) as a source of CO and as a catalyst. (*middle*) PXRD patterns of: simulated Co₂(DOBDC) (black), experimental Pd-Co₂(DOBDC) (red), experimental Pd-Co₂(DOBDC) after CO exposure (blue), experimental Pd-Co₂(DOBDC) isolated after utilization in the carbonylative Suzuki-Miyaura coupling reaction (green). (*bottom*) EDX elemental mapping analysis: SEM image of Pd-Co₂(DOBDC) and the corresponding elemental mapping for: Co, Pd, and Co and Pd.

Nitric oxide was chosen as another example of a reactive and lethal gas^[7,66-69] for adsorption in a MOF matrix and subsequent utilization as a reagent in organic reactions. Due to the reported structural stability and NO reversible adsorption capacity (6 mmol/g at 1 bar, 298 K),[37] Co₂(DOBDC) was chosen to deliver nitric oxide for carrying out the aromatization reaction of diethyl 4-ethyl-2,6-dimethyl-1,4-dihydropyridine-3,5-dicarboxylate (EDDD, Figure 6). The NO@Co2(DOBDC) sample was prepared by introducing NO gas at room temperature to the activated Co₂(DOBDC) sample, and subsequent coordination of NO molecules to the cobalt metal sites was monitored crystallographically and spectroscopically (Figures 1, 6, 8, and S10; Table S1). According to our single-crystal X-ray studies (Figure 1), the metal sites in the as-synthesized MOF were initially occupied by methanol molecules that were partially replaced by NO in the single crystals of pre-activated Co₂(DOBDC) (150 °C for 24 hours). The presence of residual methanol molecules coordinated to the metal sites was a critical drawback since it could complicate efficient NO delivery to the selected organic

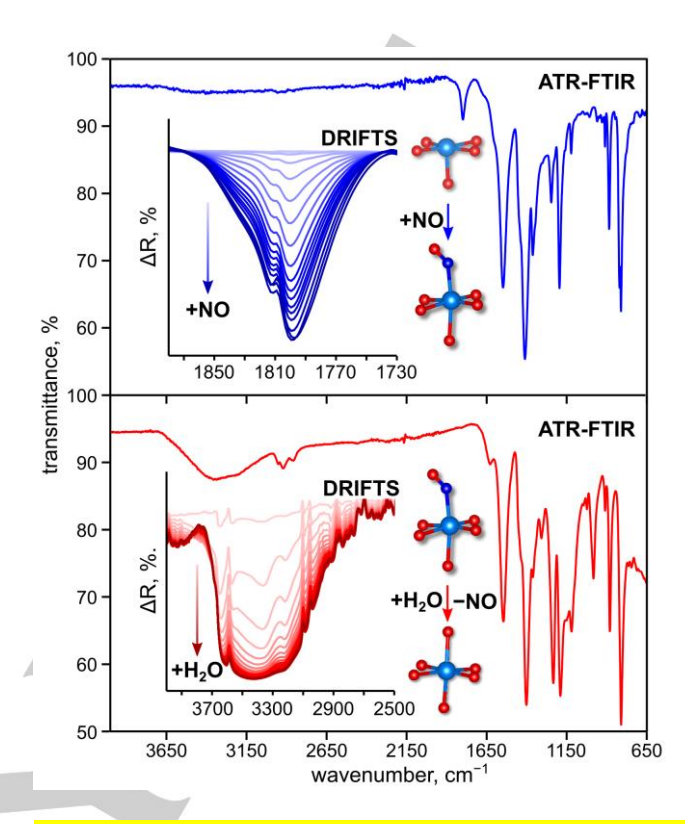


Figure 8. ATR-FTIR spectra of $NO@Co_2(DOBDC)$ before (blue) and after (red) exposure to water vapor. The insets show DRIFT spectra (% differential reflection (ΔR)) of $Co_2(DOBDC)$ during NO exposure (blue) and $NO@Co_2(DOBDC)$ during water vapor exposure (red). The light blue, dark blue, and red spheres represent cobalt, nitrogen, and oxygen atoms, respectively. Hydrogen atoms are omitted for clarity.

reactions, and therefore, we increased the MOF activation temperature from 150 °C to 180 °C. The more thorough MOF activation at 180 °C for 4 hours, followed by NO exposure, resulted in exclusive occupation of the metal sites by NO molecules, confirmed through SC-XRD studies (Figures 1 and S10; Table S1) and spectroscopic analysis (Figures 8 and S12). Notably, it is the first time that single-crystal X-ray data demonstrated direct coordination of NO molecules to the cobalt centers of the Co₂(DOBDC) framework. These findings were essential to narrow down suitable reaction conditions for efficient NO delivery using a porous matrix.

The single-crystal X-ray analysis revealed that NO bound to the MOF metal nodes were crystallographically disordered over three orientations with Co–N–O angles of 131.2(12)°, 123.2(4)°, and 119.2(7)° with an average value of 123.1(4)° (Figure S10). Similar Co–N–O angles in the range of 119.0–126.3° were also found in crystal structures of cobalt-containing organometallic complexes (Figure S13).[$^{70-72}$] Spectroscopic analysis using DRIFTS revealed a 78 cm $^{-1}$ -shift in the N–O stretching frequency to 1798 cm $^{-1}$ upon metal coordination in Co₂(DOBDC) compared to that of non-coordinated NO (1876 cm $^{-1}$),[73] which is in line with literature reports monitoring NO coordination in cobalt-based organometallic complexes and in an isostructural MOF, Fe₂(DOBDC).[36,70] DRIFTS studies were used for investigating NO@Co₂(DOBDC) for the first time (Figure 8) to demonstrate that

NO coordinated to the metal centers can be efficiently released and replaced with water molecules. Figures 8 and S11 show the disappearance of the 1798 cm⁻¹ stretching corresponding to coordinated NO molecules simultaneous growth of a broad band at 3421 cm⁻¹ corresponding to the presence of coordinated water molecules to the metal site. [74,75] Coordination of NO to the metal site is also associated with a visible color change of the material from brown (parent MOF) to black. This visible change corresponds to changes in the DR spectrum of Co₂(DOBDC) in the visible region after exposure to NO gas from two electronic transitions with λ_{max} = 580 and 720 nm to three electronic transitions with λ_{max} = 520, 600, and 700 nm (Figure S12).[36,76] This change in electronic transitions is likely related to d-d transitions, according to several literature reports.[36,76] Crystallinity of Co₂(DOBDC) was monitored by PXRD to evaluate framework integrity after NO treatment. As clearly shown in Figure 6, Co₂(DOBDC) still preserved its integrity after nitric oxide exposure.

As a model reaction for probing Co₂(DOBDC) as a nitric oxide cargo vehicle, we performed an aromatization reaction of EDDD (Figure 6). Initially, as a control experiment, we carried out EDDD aromatization using nitric oxide gas.[66-69] As reported in the literature, [66,69] introduction of trace amounts of oxygen into the system can significantly accelerate the reaction and decrease the reaction time from several hours to minutes. We applied this strategy by using atmospheric air as a readily available source of oxygen. To perform the reaction, EDDD was added to a Schlenk flask followed by its evacuation before NO (6 mL) and air (12 mL, ca. 2.5 mL oxygen) were introduced into the system. After the addition of the gaseous reagents, solvent was injected into the reaction mixture (more details in the SI) and the reaction was carried out at room temperature for 20 minutes. As a result, the conversion and yield for the formation of EDPD (EDPD = diethyl 4-ethyl-2,6-dimethylpyridine-3,5-dicarboxylate) using NO gas were found to be 100% and 97%, respectively. Carrying out the same reaction under anaerobic conditions resulted in a significantly lower yield and conversion, i.e., 43% and 31%, respectively, that is in line with literature reports emphasizing the importance of the presence of oxygen. [66,69] After probing the reaction conditions for the aromatization reaction using pure NO gas, we implemented similar conditions to perform this reaction using NO@Co2(DOBDC) as a source of NO. For that, EDDD was added to the Schlenk flask containing NO@Co2(DOBDC) under positive nitrogen pressure, and then the flask was evacuated, followed by the addition of air (as a source of oxygen). A stepwise addition was used to prevent pre-exposure of the NO@Co₂(DOBDC) sample to air. As a final step, benzene was added to the reaction mixture. The reaction was carried out at room temperature for 20 minutes (more synthetic details can be found in the SI). However, a relatively low yield of 22% for EDPD was observed. Notably, the use of pure oxygen instead of air did not lead to any significant changes in the observed yield. As expected, carrying out the same reaction under anaerobic conditions (no oxygen present) led to an even lower yield of 6%.

As shown above by our DRIFTS studies, NO molecules coordinated to the MOF metal nodes could be replaced by water molecules (Figures 8 and S11). These findings provoked us to add water to the reaction mixture under rigorous stirring, hypothesizing that the presence of water vapor could complete the release of coordinated NO molecules from the framework through water-to-nitric oxide exchange. Indeed, after the addition

of water, the gas@MOF sample, immersed in an organic solvent, changed color from black to orange. According to our DRIFTS data and literature reports, [37] this color change is indicative of the replacement of nitric oxide by water molecules, that is also supported experimentally through the observation of increased pressure inside the reaction flask. Therefore, after combining the reagents, EDDD and NO@Co2(DOBDC), and adding air and solvent, we also added 150 µL of water. The reaction was carried out at room temperature for 20 minutes (as in the case of NO gas usage; vide supra). Notably, the amount of NO anticipated to be released from the NO@MOF samples was estimated for each reaction. The product conversion and reaction yield were found to be 100% and 88%, respectively, that is in line with values obtained from using solely nitric oxide gas. Thus, even during a 20 minutes reaction duration, we were able to efficiently deliver nitric oxide to the reaction using a MOF. As a control experiment, we also carried out the same reaction in the presence of water but in the absence of oxygen (i.e., the addition of degassed water). As expected, it resulted in only 13% product conversion and 6% yield. Notably, a shortage in the amount of added oxygen (i.e., air) resulted in only a 70% conversion. Therefore, the presence of both components, oxygen and water, are critical for optimal reaction performance. Remarkably, the PXRD analysis demonstrated that Co₂(DOBDC) preserved its crystallinity after the performed treatments, including water and air addition (Figure

Conclusion

In our studies, we demonstrated that Mg- and Co-based frameworks can efficiently be used for the delivery of reactive and toxic gaseous reagents such as nitric oxide and carbon monoxide to organic reactions, while maintaining their structural integrity. On the examples of aminocarbonylation, carbonylative Suzuki-Miyaura coupling, and aromatization reactions, we probed MOFs as a cargo vehicle for reactive gases and its catalytic capabilities. We showed that, for instance, the Co-based MOF can combine functions as a gas carrier and a catalyst and be applied to carry out the carbonylative Suzuki-Miyaura coupling reaction. To the best of our knowledge, reactive (and toxic) gas delivery, especially in combination with MOF catalytic performance, were applied for the first time for exploring product formation in organic reactions. We demonstrated that in aminocarbonylation and aromatization reactions, product yields obtained from reactions using gas@MOF solid samples as reagents are comparable with yields obtained from reactions utilizing reactive carbon monoxide and nitric oxide gases. On the example of the aminocarbonylation reaction, we established that the Co₂(DOBDC) framework, isolated from the reaction mixture through gravity filtration, could be efficiently recycled for a second round of organic transformations, without sacrificing the product yield. The presented results also contain the first DRIFTS studies demonstrating CO adsorption and desorption, NO adsorption, and NO-to-water replacement in Co₂(DOBDC). In addition, the geometry of NO molecules coordinated to the MOF metal centers was resolved through single-crystal X-ray diffraction for the first time. The innovative approaches utilized in this work portend a pathway for the development of multifunctional MOF-based reagent-catalyst cargo vehicles for reactive reagents as an

conditions) on Wiley Online Library for rules of use; OA articles are governed by the applicable Creative Commons

RESEARCH ARTICLE

alternative to the use of pure toxic gases or gas generators. [46-48.77]

Acknowledgements

N.B.S. and D.A.C. gratefully acknowledge the support from the U.S. Department of Energy, Office of Science and Office of Basic Energy Sciences under Award DE-SC0019360. N.B.S. is also grateful for support from the Dreyfus Teaching-Scholar Award supported by the Dreyfus Foundation and the Hans Fischer fellowship. This material is based upon work partially supported by the National Science Foundation under Grants (S. G.) No. CHE-1955768 and No. OIA-1655740 and GEAR-CRP 20-GC03. P.K. acknowledges ASPIRE-I funding provided by the Office of the Vice President for Research, University of South Carolina.

Keywords: metal-organic frameworks • DRIFTS • nitric oxide • carbon monoxide • catalysis

- [1] R. G. Kinney, J. Tjutrins, G. M. Torres, N. J. Liu, O. Kulkarni, B. A. Arndtsen, Nat. Chem. 2018, 10, 193–199.
- [2] A. T. Lindhardt, R. Simonssen, R. H. Taaning, T. M. Gøgsig, G. N. Nilsson, G. Stenhagen, C. S. Elmore, T. Skrydstrup, *J. Label. Compd. Radiopharm.* 2012, 55, 411–418.
- [3] A. Ahlburg, A. T. Lindhardt, R. H. Taaning, A. E. Modvig, T. Skrydstrup, J. Org. Chem. 2013, 78, 10310–10318.
- [4] D. U. Nielsen, R. H. Taaning, A. T. Lindhardt, T. M. Gøgsig, T. Skrydstrup, Org. Lett. 2011, 13, 4454–4457.
- [5] D. U. Nielsen, K. Neumann, R. H. Taaning, A. T. Lindhardt, A. Modvig,T. Skrydstrup, J. Org. Chem. 2012, 77, 6155–6165.
- [6] S. Korsager, R. H. Taaning, A. T. Lindhardt, T. Skrydstrup, J. Org. Chem. 2013, 78, 6112–6120.
- [7] H. R. Ludwig, S. G. Cairelli, J. J. Whalen, Documentation for Immediately Dangerous To Life or Health Concentrations (IDLHs), Cincinnati, 1994.
- [8] R. Cao, M. R. Mian, X. Liu, Z. Chen, M. C. Wasson, X. Wang, K. B. Idrees, K. Ma, Q. Sun, J.-R. Li, T. Islamoglu, O. K. Farha, ACS Mater. Lett. 2021, 3, 1363–1368.
- [9] W. Chen, P. Cai, P. Elumalai, P. Zhang, L. Feng, M. Al-Rawashdeh, S. T. Madrahimov, H.-C. Zhou, ACS Appl. Mater. Interfaces, 2021, 13, 51849–51854.
- [10] Z. Meng, K. A. Mirica, Nano Res. 2020, 14, 369–375.
- [11] E. Velasco, Y. Osumi, S. J. Teat, S. Jensen, K. Tan, T. Thonhauser,J. Li, *Chem.* 2021, 3, 327–337.
- [12] S. Li, Y. Gao, N. Li, L. Ge, X. Bu, P. Feng, Energy Environ. Sci. 2021, 14, 1897–1927.
- [13] M. D. Allendorf, V. Stavila, M. Witman, C. K. Brozek, C. H. Hendon, J. Am. Chem. Soc. 2021, 143, 6705–6723.
- [14] M. A. Gordillo, P. A. Benavides, D. K. Panda, S. Saha, ACS Appl. Mater. Interfaces 2020, 12, 12955–12961.
- [15] H. Yang, F. Peng, D. E. Schier, S. A. Markotic, X. Zhao, A. N. Hong,
 Y. Wang, P. Feng, X. Bu, *Angew. Chem. Int. Ed.* 2021, 60, 11148–11152; *Angew. Chem.* 2021, 133, 11248–11252
- [16] K. Jayaramulu, M. E. DMello, K. Kesavan, A. Schneemann, M. Otyepka, S. Kment, C. Narayana, S. B. Kalidindi, R. S. Varma, R.

- Zboril, R. A. Fischer, J. Mater. Chem. A 2021, 9, 17434–17441.
- [17] Y. Liao, T. Sheridan, J. Liu, O. Farha, J. Hupp, ACS Appl. Mater. Interfaces 2021, 13, 30565–30575.
- [18] Y. Chen, X. Zhang, X. Wang, R. J. Drout, M. R. Mian, R. Cao, K. Ma, Q. Xia, Z. Li, O. K. Farha, J. Am. Chem. Soc. 2021, 143, 4302–4310.
- [19] M. Xu, L. Feng, L.-N. Yan, S.-S. Meng, S. Yuan, M.-J. He, H. Liang, X.-Y. Chen, H.-Y. Wei, Z.-Y. Gu, H.-C. Zhou, *Nanoscale* 2019, 11, 11270–11278.
- [20] K. Xing, R.-Q. Fan, X.-Y. Liu, S. Gai, W. Chen, Y.-L. Yang, J. Li, Chem. Commun. 2020, 56, 631–634.
- [21] X.-W. Lei, H. Yang, Y. Wang, Y. Wang, X. Chen, Y. Xiao, X. Bu, P. Feng, Small 2021, 17, 2003167.
- [22] J. L. Snider, J. Su, P. Verma, F. E. Gabaly, J. D. Sugar, L. Chen, J. M. Chames, A. A. Talin, C. Dun, J. J. Urban, V. Stavila, D. Prendergast, G. A. Somorjai, M. D. Allendorf, J. Mater. Chem. A 2021, 9, 10869–10881.
- [23] D. K. Panda, K. Maity, A. Palukoshka, F. Ibrahim, S. Saha, ACS Sustain. Chem. Eng. 2019, 7, 4619–4624.
- [24] F. Peng, H. Yang, A. Hernandez, D. E. Schier, P. Feng, X. Bu, Chem. Eur. J. 2020, 26, 11146–11149.
- [25] Z. Zhou, S. Mukherjee, S. Hou, W. Li, M. Elsner, R. A. Fischer, Angew. Chem. Int. Ed. 2021, 60, 20551–20557; Angew. Chem. 2021, 133, 20714–20721.
- [26] J. Liu, Z. Lu, Z. Chen, M. Rimoldi, A. J. Howarth, H. Chen, S. Alayoglu,
 R. Q. Snurr, O. K. Farha, J. T. Hupp, ACS Appl. Mater. Interfaces
 2021, 13, 20081–20093.
- P. M. Stanley, J. Haimerl, C. Thomas, A. Urstoeger, M. Schuster, N.
 B. Shustova, A. Casini, B. Rieger, J. Warnan, R. A. Fischer, *Angew. Chem. Int. Ed.* 2021, 60, 17854–17860; *Angew. Chem.* 2021, 133, 17998 –18004.
- [28] C. R. Martin, G. A. Leith, N. B. Shustova, Chem. Sci. 2021, 12, 7214–7230.
- [29] C. R. Martin, K. C. Park, R. E. Corkill, P. Kittikhunnatham, G. A. Leith, A. Mathur, S. L. Abiodun, A. B. Greytak, N. B. Shustova, *Faraday Discuss.*, 2021, 231, 266–280.
- [30] C. R. Martin, P. Kittikhunnatham, G. A. Leith, A. A. Berseneva, K. C. Park, A. B. Greytak, N. B. Shustova, *Nano Res.* 2021, 14, 338–354.
- [31] A. M. Rice, C. R. Martin, V. A. Galitskiy, A. A. Berseneva, G. A. Leith,
 N. B. Shustova, *Chem. Rev.* 2019, 120, 8790–8813.
- [32] M. Bornstein, D. M. Parker, A. D. Quast, J. S. Shumaker-Parry, I. Zharov, ChemCatChem 2019, 11, 4360–4367.
- [33] E. V. Dikarev, D. K. Kumar, A. S. Filatov, A. Anan, Y. Xie, T. Asefa, M. A. Petrukhina, *ChemCatChem* **2010**, *2*, 1461–1466.
- [34] E. D. Bloch, M. R. Hudson, J. A. Mason, S. Chavan, V. Crocellà, J.
 D. Howe, K. Lee, A. L. Dzubak, W. L. Queen, J. M. Zadrozny, S. J.
 Geier, L.-C. Lin, L. Gagliardi, B. Smit, J. B. Neaton, S. Bordiga, C. M.
 Brown, J. R. Long, J. Am. Chem. Soc. 2014, 136, 10752–10761.
- [35] M. I. Gonzalez, J. A. Mason, E. D. Bloch, S. J. Teat, K. J. Gagnon, G. Y. Morrison, W. L. Queen, J. R. Long, *Chem. Sci.* **2017**, *8*, 4387–4398.
- [36] E. D. Bloch, W. L. Queen, S. Chavan, P. S. Wheatley, J. M. Zadrozny,
 R. Morris, C. M. Brown, C. Lamberti, S. Bordiga, J. R. Long, *J. Am. Chem. Soc.* 2015, 137, 3466–3469.
- [37] A. C. McKinlay, B. Xiao, D. S. Wragg, P. S. Wheatley, I. L. Megson,
 R. E. Morris, J. Am. Chem. Soc. 2008, 130, 10440–10444.
- [38] Y. Zhou, T. Yang, K. Liang, R. Chandrawati, *Adv. Drug Deliv. Rev.* 2021, 171, 199–214.

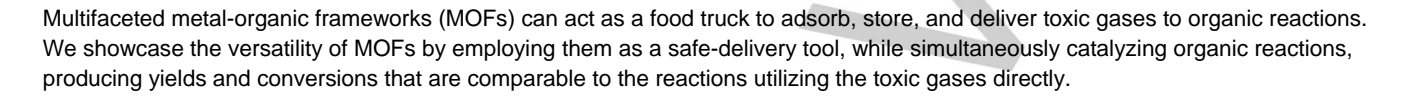
RESEARCH ARTICLE

- [39] D. Cattaneo, S. J. Warrender, M. J. Duncan, C. J. Kelsall, M. K. Doherty, P. D. Whitfield, I. L. Megson, R. E. Morris, RSC Adv. 2016, 6, 14059–14067.
- [40] B. Xiao, P. S. Wheatley, X. Zhao, A. J. Fletcher, S. Fox, A. G. Rossi,
 I. L. Megson, S. Bordiga, L. Regli, K. M. Thomas, R. E. Morris, *J. Am. Chem. Soc.* 2007, *129*, 1203–1209.
- [41] S. Diring, A. Carné-Sánchez, J. Zhang, S. Ikemura, C. Kim, H. Inaba, S. Kitaqawa, S. Furukawa, Chem. Sci. 2017, 8, 2381–2386.
- [42] W.-P. Li, C.-H. Su, L.-C. Tsao, C.-T. Chang, Y.-P. Hsu, C.-S. Yeh, ACS Nano 2016, 10, 11027–11036.
- [43] Z. Jin, P. Zhao, J. Zhang, T. Yang, G. Zhou, D. Zhang, T. Wang, Q. He. Chem. Eur. J. 2018. 24, 11667–11674.
- [44] D. Ribatti, A. Vacca, Leuk. 2005, 19, 1525–1531.
- [45] F. Cavallo, M. Boccadoro, A. Palumbo, Ther. Clin. Risk Manag. 2007, 3. 543-552.
- [46] X.-F. Wu, S. Oschatz, M. Sharif, A. Flader, L. Krey, M. Beller, P. Langer, Adv. Synth. Catal. 2013, 355, 3581–3585.
- [47] S.-W. Tao, R.-Q. Liu, J.-Y. Zhou, Y.-M. Zhu, ChemistrySelect 2020, 5, 7332–7337.
- [48] C. Shao, A. Lu, X. Wang, B. Zhou, X. Guan, Y. Zhang, Org. Biomol. Chem. 2017, 15, 5033–5040.
- [49] F. J. Carmona, S. Rojas, C. C. Romão, J. A. R. Navarro, E. Barea, C. R. Maldonado, Chem. Commun. 2017, 53, 6581–6584.
- [50] F. J. Carmona, C. R. Maldonado, S. Ikemura, C. C. Romão, Z. Huang, H. Xu, X. Zou, S. Kitagawa, S. Furukawa, E. Barea, ACS Appl. Mater. Interfaces 2018, 10, 31158–31167.
- [51] S. R. Caskey, A. G. Wong-Foy, A. J. Matzger, J. Am. Chem. Soc. 2008, 130, 10870–10871.
- [52] P. D. C. Dietzel, R. Blom, H. Fjellvåg, Eur. J. Inorg. Chem. 2008, 2008, 3624–3632.
- [53] P. D. C. Dietzel, Y. Morita, R. Blom, H. Fjellvåg, Angew. Chem. Int. Ed. 2005, 44, 6354–6358; Angew. Chem. 2005, 117, 6512-6516.
- [54] J. Frafjord, I. G. Ringdalen, O. S. Hopperstad, R. Holmestad, J. Friis, Comput. Mater. Sci. 2020, 184, 109902.
- [55] M. V. Parkes, D. F. S. Gallis, J. A. Greathouse, T. M. Nenoff, J. Phys. Chem. C 2015, 119, 6556–6567.
- [56] A. A. Yakovenko, J. H. Reibenspies, N. Bhuvanesh, H.-C. Zhou, J. Appl. Cryst. 2013, 46, 346–353.
- [57] R. H. Crabtree, The Organometallic Chemistry of the Transition Metals: Sixth Edition, Wiley Blackwell, 2014.
- [58] S. Chavan, J. G. Vitillo, E. Groppo, F. Bonino, C. Lamberti, P. D. C. Dietzel, S. Bordiga, J. Phys. Chem. C 2009, 113, 3292–3299.
- [59] H. Kim, M. Sohail, K. Yim, Y. C. Park, D. H. Chun, H. J. Kim, S. O. Han, J.-H. Moon, ACS Appl. Mater. Interfaces 2019, 11, 7014–7021.
- [60] W. L. Queen, M. R. Hudson, E. D. Bloch, J. A. Mason, M. I. Gonzalez, J. S. Lee, D. Gygi, J. D. Howe, K. Lee, T. A. Darwish, M. James, V. K. Peterson, S. J. Teat, B. Smit, J. B. Neaton, J. R. Long, C. M. Brown, Chem. Sci. 2014, 5, 4569–4581.
- [61] W. R. Heinz, I. Agirrezabal-Telleria, R. Junk, J. Berger, J. Wang, D. I. Sharapa, M. Gil-Calvo, I. Luz, M. Soukri, F. Studt, Y. Wang, C. Wöll, H. Bunzen, M. Drees, R. A. Fischer, ACS Appl. Mater. Interfaces 2020, 12, 40635–40647.
- [62] W. R. Heinz, T. Kratky, M. Drees, A. Wimmer, O. Tomanec, S. Günther, M. Schuster, R. A. Fischer, Dalt. Trans. 2019, 48, 12031–12039.
- [63] G. Nickerl, U. Stoeck, U. Burkhardt, I. Senkovska, S. Kaskel, J. Mater. Chem. A 2014, 2, 144–148.

- [64] D. M. Shakya, O. A. Ejegbavwo, T. Rajeshkumar, S. D. Senanayake, A. J. Brandt, S. Farzandh, N. Acharya, A. M. Ebrahim, A. I. Frenkel, N. Rui, G. L. Tate, J. R. Monnier, K. D. Vogiatzis, N. B. Shustova, D. A. Chen, Angew. Chem. Int. Ed. 2019, 58, 16533–16537; Angew. Chem. 2019, 131, 16685-16689.
- [65] R. S. Salama, M. A. Mannaa, H. M. Altass, A. A. Ibrahim, A. E.-R. S. Khder, RSC Adv. 2021, 11, 4318–4326.
- [66] T. Itoh, K. Nagata, M. Okada, A. Ohsawa, *Tetrahedron Lett.* 1995, 36, 2269–2272.
- [67] B. Loev, K. M. Snader, J. Org. Chem. 1965, 30, 1914–1916.
- [68] X.-Q. Zhu, B.-J. Zhao, J.-P. Cheng, J. Org. Chem. 2000, 65, 8158– 8163
- [69] T. Itoh, K. Nagata, Y. Matsuya, M. Miyazaki, A. Ohsawa, J. Org. Chem. 1997, 62, 3582–3585.
- [70] M. K. Ellison, W. R. Scheidt, Inorg. Chem. 1998, 37, 382–383.
- [71] C. S. Pratt, B. A. Coyle, J. A. Ibers, J. Chem. Soc. A 1971, 2146– 2151
- [72] L. F. Larkworthy, D. C. Povey, J. Crystallogr. Spectrosc. Res. 1983, 13, 413–420.
- [73] R. R. Smardzewski, W. B. Fox, J. Chem. Phys. 1974, 60, 2104.
- [74] S. Packiaraj, M. Jeyaraj, K. Chandarasekaran, J. M. Rawson, S. Govindarajan, J. Mater. Sci. Mater. Electron. 2019, 30, 18866–18877.
- [75] K. Tan, S. Zuluaga, Q. Gong, Y. Gao, N. Nijem, J. Li, T. Thonhauser, Y. J. Chabal, Chem. Mater. 2015, 27, 2203–2217.
- [76] I. Strauss, A. Mundstock, D. Hinrichs, R. Himstedt, A. Knebel, C. Reinhardt, D. Dorfs, J. Caro, *Angew. Chem. Int. Ed.* 2018, 57, 7434–7439; *Angew. Chem.* 2018, 130, 7556–7561.
- [77] S. D. Friis, A. T. Lindhardt, T. Skrydstrup, Acc. Chem. Res. 2016, 49, 504–605
- [78] Deposition Numbers 2108214, 2108215, and 2108216 contain the supplementary crystallographic data for this paper. These data can be obtained free of charge from The Cambridge Crystallographic Data Centre at www.ccdc.cam.ac.uk/structures.

Entry for the Table of Contents





Institute and/or researcher Twitter usernames: ShustovaLab

